Zou, Fangxin; Cucharero, Jose; Dong, Yujiao; Kangas, Pinja; Zhu, Ya; Kaskirinne, Janne; Tewari, Girish C.; Hänninen, Tuomas; Lokki, Tapio; Li, Hailong; Vapaavuori, Jaana

# Maximizing sound absorption, thermal insulation, and mechanical strength of anisotropic pectin cryogels

*Published in:*
Chemical Engineering Journal

*DOI:*
10.1016/j.cej.2023.142236

Published: 15/04/2023

*Document Version*
Publisher's PDF, also known as Version of record

Chemical Engineering Journal 462 (2023) 142236

Contents lists available at ScienceDirect

Chemical Engineering Journal

journal homepage: www.elsevier.com/locate/cej

# Maximizing sound absorption, thermal insulation, and mechanical strength of anisotropic pectin cryogels

Fangxin Zou [a], Jose Cucharero [b,e], Yujiao Dong [a], Pinja Kangas [a], Ya Zhu [c], Janne Kaskirinne [a], Girish C. Tewari [a], Tuomas Hänninen [e], Tapio Lokki [b], Hailong Li [d,*], Jaana Vapaavuori [a,*]

[a] Department of Chemistry and Materials Science, Aalto University, Kemistintie 1, 02150 Espoo, Finland
[b] Acoustics Lab, Department of Information and Communications Engineering, School of Electrical Engineering, Otakaari 5E, 00076 Espoo, Finland
[c] Department of Bioproducts and Biosystems, Aalto University, Vuorimiehentie 1, 02150 Espoo, Finland
[d] State Key Laboratory of Fine Chemicals, School of Chemical Engineering, Dalian University of Technology, 116024 Dalian, China
[e] Lumir Oy, 01260 Vantaa, Finland

ARTICLE INFO

*Keywords:*
Pectin cryogels
Freeze-casting
Hierarchically porous structure
Sound absorption
Thermal insulation

ABSTRACT

Effective use of sound absorption materials is the main way to reduce noise pollution, which constitutes a major environmental and health problem. However, the currently used porous sound absorption materials cause not only environmental pollution but their usage is also a potential health risk. Here, we demonstrate a facile strategy to create environmental-friendly and non-toxic lightweight pectin-based cryogels with hierarchically porous anisotropic structure, which integrates small pores on the walls of lamellar pores, via freeze-casting method. The fabricated pectin cryogels have better sound absorption performance (average sound absorption coefficient up to 0.76 in 500–6000 Hz), higher compression modulus (300 to 700 times higher than commercial glass wool), and comparable thermal conductivity comparing to other reported bio-based porous materials. Moreover, the sound absorption performance could be enhanced and optimized by tuning the pore wall density of lamellar pores and the size of small pores to the level of viscous and thermal layers via increasing of freeze-casting temperature and adding NaCl in pectin solution prior to the freeze-casting process. The outstanding sound absorption is linked to the unique hierarchically porous morphology of these cryogels. This strategy paves the way for the design of bio-based porous anisotropic materials for highly efficient noise absorption.

## 1. Introduction

Nowadays, noise pollution creates major environmental and health problems due to the expansion of industry, urbanization, and transportation. Noise-related severe physical and mental health problems can include sleep disturbances, hearing damage, hypertension, and inattention [1]. The main way to counteract the problems caused by noise pollution is the effective use of sound absorption materials [2]. Among them, porous sound absorption materials have gained attention due to their wide sound absorption frequency range compared to the resonant sound absorption materials [3]. The most commonly used sound absorbing porous materials during the past few decades can be classified into two types: fibrous materials [4,5] which are fabricated out of glass fiber [6] or other mineral fibers [7], and synthetic polymers-based foam [3,8] (such as melamine foam [9] and polyurethane foam [10,11]). Unfortunately, these two types of porous sound absorption materials not only cause environmental pollution during their preparation and use, but also can cause health risks and safety issues for humans [12].

Motivated by the request of green societal transition, using biodegradable, biocompatible, and non-toxic natural raw materials to fabricate porous sound absorbers has drawn an arising attention. In recent years, various types of natural raw materials, such as wood pulp [13], coir fibers [14], natural kenaf fiber [12], and cellulose [15] have been used to fabricated bio-based porous sound absorption materials. However, most of the net bio-based porous materials have poor mechanical properties and additional reinforcing components are needed to increase their mechanical performance [16,17].

To improve the mechanical strength and reduce the usage of other components (such as inorganic particles [17]) in the bio-based porous materials, a new fabrication method, freeze-casting, was established. Freeze-casting is an outstanding technique to fabricate porous ceramic, synthetic polymer, and metal materials, called cryogels, with highly

* Corresponding authors.
*E-mail addresses:* lihailong@dlut.edu.cn (H. Li), jaana.vapaavuori@aalto.fi (J. Vapaavuori).

https://doi.org/10.1016/j.cej.2023.142236
Received 24 October 2022; Received in revised form 30 January 2023; Accepted 28 February 2023
Available online 3 March 2023

aligned anisotropic structure by controlling ice growth direction during freezing [18,19]. The resulting anisotropic porous materials not only have light weight and high porosity but also exhibit excellent compression modulus along the ice growth direction [20,21]. The high compression resistance was interpreted to be due to the deformation occuring through the pore wall's plastic bending [22]. Consequently, various types of bio-based cryogels with impressive mechanical properties have been fabricated in recent years [23–28]. For example, pectin as an inexpensive and abundant polysaccharide, which can be extracted from plant cell wall [29], has been reported as a raw material to fabricate anisotropic porous materials, which can be used as liquid transport device [20] or as a template for pectin/poly(methyl methacrylate) (PMMA) composite [30] with high optical transmittance, good UV blocking ability, and low thermal conductivity. However, to the best of our knowledge, only few types of polysaccharides, cellulose II [31] and chitosan [32], have been reported as the raw materials to fabricate freeze-casted sound absorption porous materials. Therefore, exploring the potential of the freeze-casted cryogels prepared from pectin as sustainable and economically viable sound absorption materials can open an opportunity for pectin to expand its industrial value as a food industry byproduct, and at the same time, increase the sustainability of sound absorption materials fabrication by establishing new circular economy approaches.

In the present study, the possibility of using pectin-based anisotropic cryogels fabricated via freeze-casting method as sound absorption materials and the controllability of the final cryogel morphology through salt addition were investigated. In order to study the influence of morphologies of pectin cryogels on the sound absorption performance, three freeze-casting media with different temperatures (-20 °C, −79 °C, −196 °C) and various concentrations of sodium chloride (NaCl) added into pectin solution prior to the freeze-casting process were used. Sound absorption coefficient in frequency range of 500–6000 Hz, mechanical properties under uniaxial compression, and thermal conductivity were investigated and compared with other porous materials reported in the literature. The freeze-casted pectin cryogels have high compression modulus, low thermal conductivity, and excellent sound absorption property which could also be enhanced and tailored by adjusting the NaCl concentration. More importantly, we were able to find conditions for producing a cryogel that outperforms the commercial standard materials in acoustic absorption. Overall, these materials provide a promising alternative to be employed in sound absorption and can thus contribute towards adoption of environmentally-friendly strategies in the construction field.

## 2. Experimental section/methods

### 2.1. Materials

Pectin from citrus peel and sodium chloride (NaCl, 99%) were purchased from Sigma-Aldrich. All chemicals were used without any further purification. Distillated water was used to dissolve pectin and NaCl.

### 2.2. Preparation of freeze-casted pectin cryogels

Pectin cryogels were prepared according to our previous work [30] and with the following steps as illustrated in Fig. 1. NaCl solutions with various concentrations (0 M, 0.01 M, 0.05 M, 0.1 M, and 0.2 M) were prepared by dissolving NaCl in distilled water at room temperature under magnetic stirring. Pectin (its chemical structure shown in Fig. S1) powders were dissolved in the prepared NaCl solutions with pectin dry concentration of 3 wt% under magnetic stirring for 24 h at room temperature. Then, the prepared pectin solution was poured into Teflon mold with copper plate as bottom at room temperature. After that, the Teflon mold was transferred to and placed in the low temperature bath, which was filled with either dry ice (−79 °C) or liquid nitrogen (-196 °C), or directly placed on cold copper plate which storage in the fridge at the temperature of −20 °C to get freeze-casted frozen gel. All the frozen gels were then freeze-dried for 7 days by the Alpha 2–4 LSCbasic freeze dryer (Martin Christ Gefriertrocknungsanlagen GmbH) to obtain pectin cryogels. The obtained pectin cryogels are named as "N-X M", where N is the freezing source (−20 °C, dry ice or liquid nitrogen) and X is the concentration of NaCl. For easy illustration, the direction along and across the ice growth direction was named as axial and radial direction, respectively.

### 2.3. Characterization

#### 2.3.1. Scanning electron microscope (SEM)

The morphologies of freeze-casted pectin cryogels were characterized by Scanning Electron Microscope (TESCAN MIRA 3). Before the measurement, sample's surface was coated by a thin Au/Pd (80/20) layer with Q150T coater (Quorum). The cryogels' pore wall density which is based on the number of pore walls in 1 mm and pore size of pores formed on the lamellar pore wall were measured from SEM images by using ImageJ software.

#### 2.3.2. Bulk density and porosity

Bulk density ($\rho_b$), porosity, and linear shrinkage of freeze-casted pectin cryogels were calculated as follows:

$$\rho_b = \frac{m}{V} \tag{1}$$

$$\text{porosity} = \frac{\rho_s - \rho_b}{\rho_s} \times 100\% \tag{2}$$

$$\text{linear shrinkage} = \frac{R_f - R_d}{R_f} \times 100\% \tag{3}$$

where $m$ and $V$ are the sample's weight and volume, respectively. $\rho_s$ is the skeletal density of pectin networks [33] ($\rho_s = 1.5$ g/cm$^3$). $R_f$ and $R_d$ are the sample's diameter before and after drying, respectively. Sample's weight, volume, and diameter were measured for 4 times to obtain the average value.

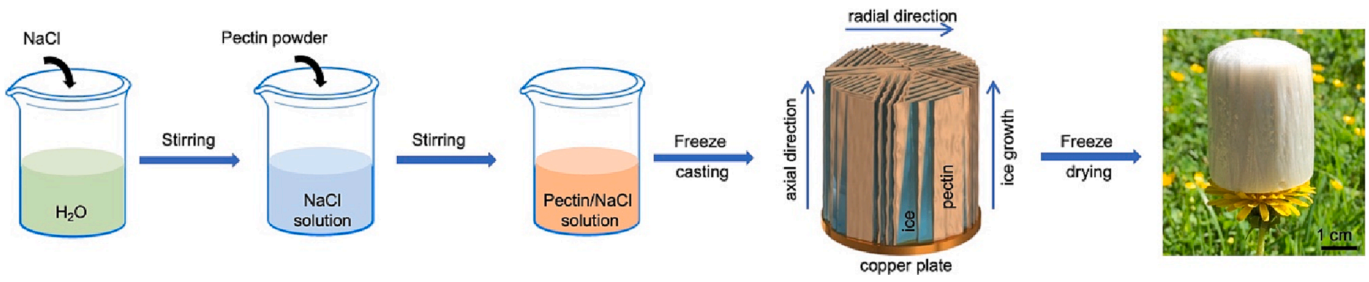


**Fig. 1.** Schematic illustration of the processing routes to prepare freeze-casted pectin cryogels with different freezing sources and NaCl concentrations. The digital photo of the freeze-casted pectin cryogel placed on a flower is presented on the right. Its density is 0.035 g/cm$^3$.

#### 2.3.3. Sound absorption performance

The normal sound absorption coefficients of freeze-casted pectin cryogels were measured using an impedance tube (Brüel & Kjær Type 4206) according to the transfer-function method defined in the standard (ISO 10534-2 1998). The sample diameter was 29 mm and thickness were varied form 12 mm to 30 mm (cut across the ice growth direction). The measured frequency ranges from 500 to 6000 Hz and the 1/3 octave frequency bands (500, 630, 800, 1000, 1250, 1600, 2000, 2500, 3150, 4000, 5000, and 6000 Hz) were taken and used to plot the sound absorption coefficient curves. Each sample was measured at least 3 times to minimize the error. The average absorption coefficient is the average of the sound absorption coefficients at 500, 630, 800, 1000, 1250, 1600, 2000, 2500, 3150, 4000, 5000, and 6000 Hz and it also be used to evaluate the sound absorption performance.

#### 2.3.4. Mechanical property

The mechanical property of freeze-casted pectin cryogel under uniaxial compression in the axial direction was measured by using universal tester Instron 4204 equipped with a 100 N load cell. All samples were cut into cubes of around 1 $cm^3$ in size and compressed with a constant compression rate of 1 mm/min. All measurements were repeated for 4 or 5 times.

#### 2.3.5. Thermal insulation capacity

The thermal conductivity measurements were performed on Physical Property Measurement System (PPMS DynaCool, Quantum Design) at 30 °C. Carbon tape was used to attach the pectin cryogel in between two copper chips. The thermal conductivity was measured at isothermal condition. The temperature difference was measured between two faces of the pectin cryogel when the steady-state was reached. The thermal conductivity could be calculated by using sample's dimensions (length, width, and thickness) and temperature difference of sample's two faces. The temperature depends of thermal conductivity were measured in temperature ranges from −22 °C to 105 °C. The thermal insulation performance of pectin cryogel during heating or cooling was conducted by putting a 12 mm thick or 30 mm thick sample on a 100 °C hot plate or −79 °C cold plate. The surface temperature of each sample during the heating or cooling process was recorded every 5 s by an infrared camera (PIR uc 180, InfraTec), which has a lowest detection temperature of −35 °C.

## 3. Results and discussion

In order to understand the influence of freezing media and NaCl concentration on the morphology of final freeze-casted pectin cryogels, a large library of samples was prepared, and the corresponding SEM images are shown in Fig. 2a-f'' and Fig. S2 and S3. All pectin cryogels frozen with liquid nitrogen (−196 °C) and dry ice (−79 °C) have anisotropic structures with porous structure in radial direction (Fig. 2a-f, cut across the ice growth direction) and parallel lamellar structure in axial direction (Fig. 2a'-f', cut along the ice growth direction). This is due to the directional growth of ice controlled by temperature gradient direction during freeze-casting process [18,19]. By changing the freezing source from liquid nitrogen to dry ice and when increasing the NaCl concentration, the pore size increases and the gap between two lamellar pore walls becomes wider. Similar results were reported by Wu et al. for pure water, where the pore size of ice increases when adding salt to water [34]. Thus, both the freezing source and NaCl concentration have influences on the morphology. Surprisingly, small pores were observed on the walls of the parallel lamellar structures (Fig. 2a''-f'' and Fig. S3). This might be related to several reasons during the freezing process, including the ability to form a uniform pore wall, the diversity of ice crystals' size and shape, and so on. The size of those small pores increases when increasing the NaCl concentration (Fig. 3a and Fig. S4). The total number of those small pores first increases and then decreases with increasing the NaCl concentration (Fig. S3). This might be due to the ability to form a uniform pore wall, which decreases with the increase of NaCl concentration. Therefore, the number of small pores increases at moderate NaCl concentrations. However, when NaCl concentration is further increased, the large amount of small pores can combine into bigger pores resulting in the decrease of the overall number of pores.

To elucidate the effect of freezing source and NaCl concentration on freeze-casted pectin cryogels, their density, porosity, and pore wall density are summarized in Fig. 3b-d. It is clearly observed that the density (porosity) of the cryogels increases (decreases) very slightly when NaCl concentration is lower than 0.05 M. While above 0.05 M, a large increase (decrease) was observed for the density (porosity) of the

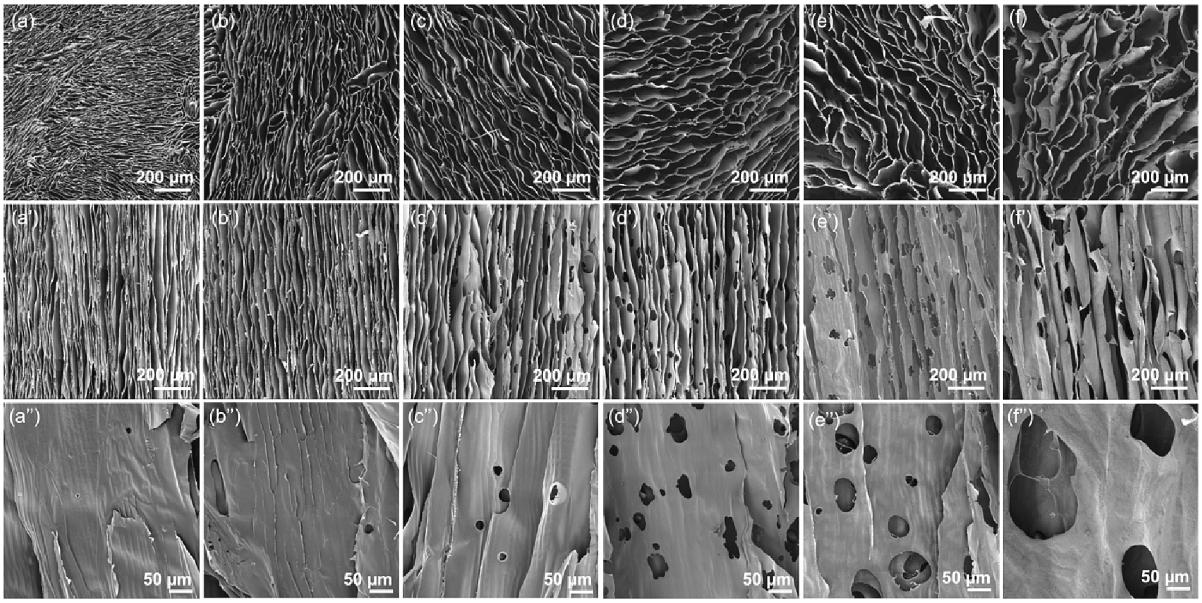


**Fig. 2.** SEM images of freeze-casted pectin cryogels prepared with different freezing sources and NaCl concentrations (cut across (a-f), along (a'-f') the ice growth direction, and high magnification SEM images of pectin cryogel's pore wall (a''-f''), respectively): (a,a',a'') liquid nitrogen-0 M, (b,b',b'') dry ice-0 M, (c,c',c'') dry ice-0.01 M, (d,d',d'') dry ice-0.05 M, (e,e',e'') dry ice-0.1 M, and (f,f',f'') dry ice-0.2 M.

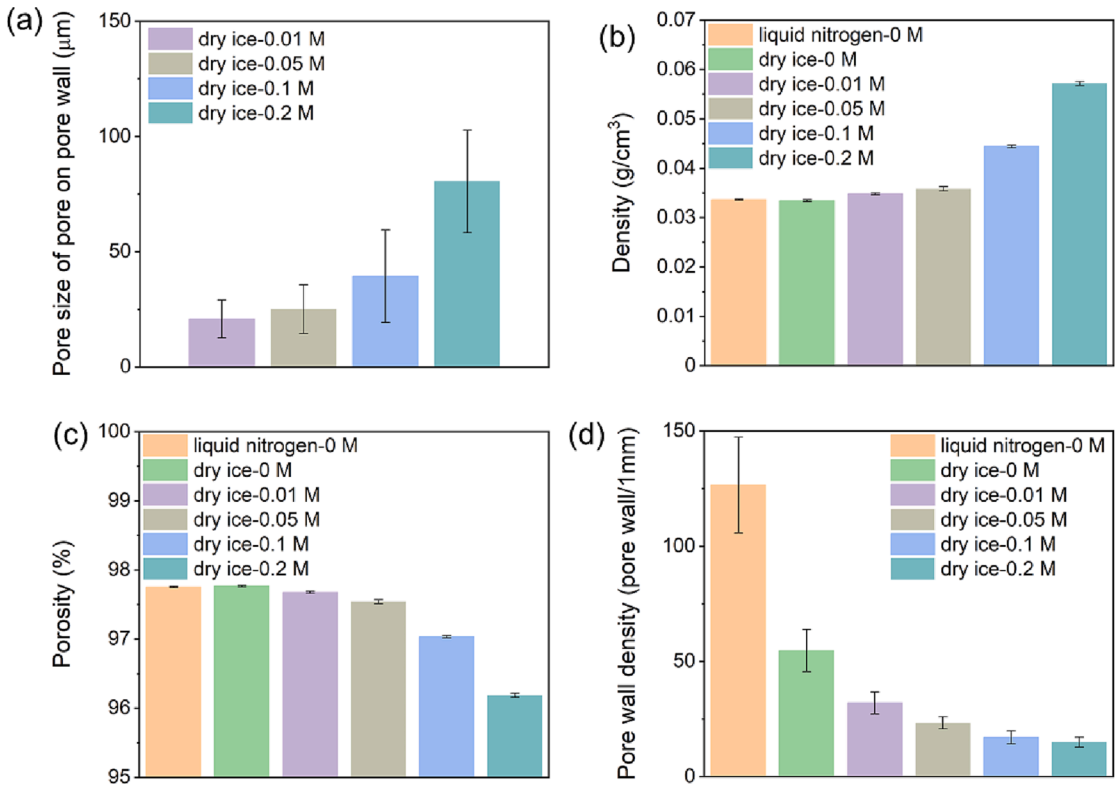


**Fig. 3.** Pore size of small pores on the lamellar pore wall (a), density (b), porosity (c), and pore wall density (d) of freeze-casted pectin cryogels prepared with different freezing sources and NaCl concentrations.

cryogels when increasing the NaCl concentration (Fig. 3b,c). This result is most likely caused by two reasons: firstly, addition of NaCl into the solution increases the total weight of the prepared cryogel sample; secondly, the linear shrinkage of the cryogel's diameter upon freeze-drying has a significant increase from 8% to 14% when the NaCl concentration is increased from 0.05 M to 0.2 M (Fig. S5), which might be related to the increasing pore size of the pores on the parallel lamellar structures with the consequence of a decreasing mechanical strength of the parallel lamellar structures. Hence, for dry ice-0.2 M cryogel, the density is much higher as compared to other samples, while the porosity only decreases very slightly from 97.8% to 96.2% (Fig. 3c).

Pore wall density is frequently used as a parameter to reflect the pore size of materials with anisotropic and lamellar structures. In this work, pore wall density of cryogels was calculated by counting the numbers of pore wall within 1 mm distance on the SEM images (Fig. 2a'-f') and summarized in Fig. 3d. It is observed that freezing source and NaCl concentration highly affect the pore wall density. The pectin cryogel prepared by freeze-casting with dry ice has much lower pore wall density (55 pore walls/mm) than that of liquid nitrogen freeze-casted cryogel (127 pore walls/mm). This is due to the smaller number of ice nucleates formed at much higher freezing temperature with dry ice (−79 °C) than when freezing with liquid nitrogen (−196 °C). It is consistent with the reported freeze-casted pectin cryogels [20,30]. Overall, this result suggests that smaller temperature gradient results in a lower pore wall density.

Additionally, by adding NaCl into the pectin solution the pore wall density of pectin cryogels frozen by dry ice could be decreased from 55 to 15 pore walls/mm, when increasing the NaCl concentration from 0 M to 0.2 M (Fig. 3d). From the rheology results in Fig. S6, it is observed that the viscosity of pectin solutions increases only very slightly when adding NaCl (Fig. S6), and changes in rheological properties are thus not expected to be the dominant cause for the large decrease of pore wall density. On the other hand, it is well known that the freezing point of water decreases upon salt addition. Therefore, when freeze-casting the pectin/NaCl/water solutions the temperature gradient is smaller than that of pectin/water solutions, leading to a lower pore wall density cryogel. This result further supports the conclusion that smaller temperature gradient results in a lower pore wall density. When further increasing the freeze-casting temperature to −20 °C by changing the freezing media, the final pectin cryogel has isotropic structure with random pore structures instead of the anisotropic structure (Fig. S2). This suggests that a sufficient temperature gradient is a key parameter for the forming of anisotropic structures via controlling the number of ice nucleates and ice growth rate. When the temperature gradient is not large enough the anisotropic structures will not form at all [20].

Due to their high porosity, the prepared pectin cryogels have great potential to be used as sound absorption materials. First, the effect of the cryogel morphology on the sound absorption performance of pectin cryogels was investigated. The sound absorption coefficients of pectin cryogels prepared with freeze-casting at different temperatures and with different added NaCl concentrations were measured via a sound impedance tube and shown in Fig. 4a. Common commercial sound absorption material, glass wool, with density of 0.05 g/cm$^3$, was measured as a reference. For the glass wool, its sound absorption coefficient increases as a function of frequency of the sound wave. For pectin cryogels, the sound absorption coefficient depends not only on the sound frequency but also on the preparation parameters (freezing temperature and NaCl concentration). The first absorption peak of the dry ice freeze-casted pectin cryogels prepared from lower (<0.01 M) NaCl concentration was observed at lower frequencies, at around 1000 Hz. This may be related to higher pore wall density (equaling small lamellar pore size) resulting in higher flow resistance at the low frequency with longer wavelength [35]. Increasing NaCl concentration to 0.05 M results in lower absorption properties below 2000 Hz but greater absorption above this frequency. The increase in NaCl concentration from 0.05 M to 0.1 M did not lead to significant variations in the absorption properties of the cryogels. When the NaCl concentration was increased to 0.2 M the similar shape of absorption spectra as for concentrations of 0.05 M and

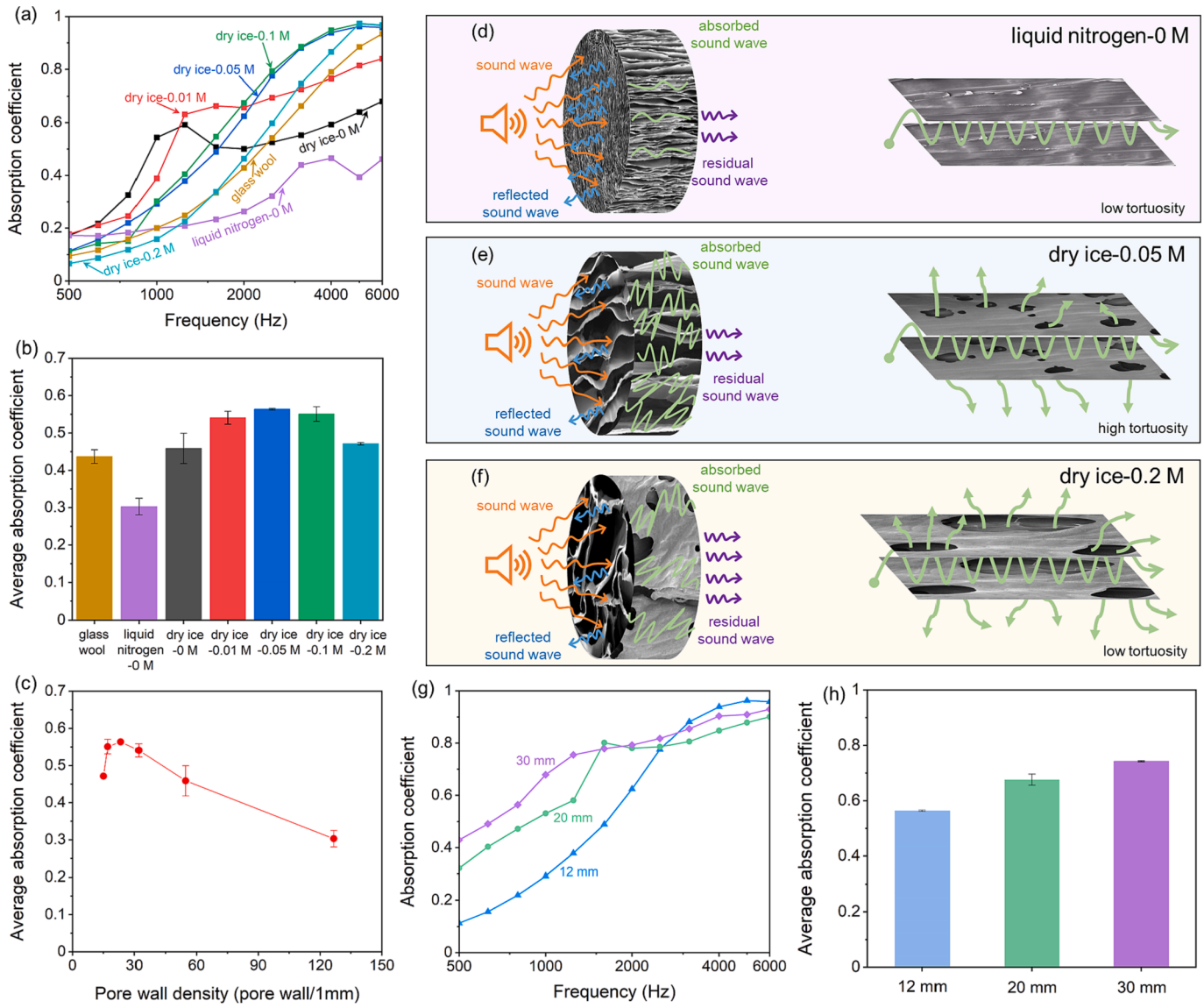


**Fig. 4.** Absorption coefficient (a) and average absorption coefficient (b) of 12 mm thick pectin cryogels prepared with different freezing sources and NaCl concentrations. 0.05 g/cm$^3$ glass wool was used as reference. (c) Pore wall density dependent of average absorption coefficient. Schematic illustrations of the mechanisms of the sound absorption for liquid nitrogen-0 M (d), dry ice-0.05 M (e), and dry ice-0.2 M (f) samples: The left graph in each Figure is to show how the sound waves can be reflected, absorbed or transmitted by materials, when sound waves strike the materials, whereas the right graph in each Figure illustrates the dissipation of sound by tortuosity of the structure. The influence of thickness on the absorption coefficient (g) and the average absorption coefficient (h) of dry ice-0.05 M pectin cryogels.

0.1 M was retained, however, the absorption coefficient decreases gradually for the frequencies below 5000 Hz.

The liquid nitrogen freeze-casted pectin cryogel prepared without adding NaCl has better sound absorption property compared to glass wool only in the lower frequency range (500–1000 Hz). In contrast, the advantages of pectin cryogels with increased freeze-casting temperature and NaCl concentration are extended to higher frequency and wider frequency range as compared to glass wool. For example, the dry ice-0 M sample has a higher sound absorption coefficient in frequency 500–2400 Hz, and the dry ice-0.05 M sample exhibits a higher sound absorption coefficient in the full measured frequency ranges (500–6000 Hz) compared with glass wool. However, if further increasing the NaCl concentration to 0.2 M, the sound absorption coefficient will be decreased, still outperforming glass wool in the frequency range of 1600–6000 Hz. Interestingly, for the dry ice freeze-casted pectin cryogels, their sound absorption coefficient increases with the NaCl concentration in the higher frequency range but decreases in the lower frequency range (Fig. 4a). These results indicate that the working frequency of pectin cryogels could be adjusted by changing the NaCl concentration.

The average sound absorption coefficient in the frequency range from 500 to 6000 Hz can be used to evaluate the general sound absorption ability of these cryogels to absorb noise from industry, urbanization, and transportation [36]. As shown in Fig. 4b, the average sound absorption coefficient increases from 0.30 to 0.46 when increasing the freeze-casting temperature by changing the freezing media from liquid nitrogen to dry ice, which is only slightly higher than that of glass wool at 0.44. With the adding of a little amount of NaCl, such as dry ice-0.01 M, a noteworthy increase in the average sound absorption coefficient of 0.54 was observed rendering it much higher than that of glass wool. The average sound absorption coefficient was further increased to 0.56 when increasing the NaCl concentration to 0.05 M. However, when NaCl concentration was higher than 0.05 M the average sound absorption coefficient starts to saturate (0.55) for dry ice-0.1 M and decreases to

0.47 for dry ice-0.2 M. This result clearly suggested that there is an upper limit of improving the sound absorption property of pectin cryogels by increasing NaCl concentration. This conclusion is directly illustrated by the pore wall density dependence of average absorption coefficient, plotted in Fig. 4c. The maximum average absorption coefficient was obtained from the dry ice-0.05 M cryogel which have a pore wall density of 23 pore walls/mm.

Based on the morphology results in Fig. 2, the most probable reason for the enhanced sound absorption performance of pectin cryogels prepared by increasing freeze-casting temperature and NaCl concentration can be explained by the pore wall density and the size of the small pores on the parallel lamellar pore wall. With low freezing temperature and low NaCl concentration, for example liquid nitrogen-0 M, there are lots of small parallel lamellar pores meaning higher pore wall density (see Fig. 3d) and no small pores on the wall (see Fig. 2a"). Thus, a larger portion of sound energy was reflected by the cryogel surface; only a small amount of sound wave penetrated the cryogel, most of which was dissipated (Fig. 4d). With high freezing temperature and NaCl concentration, for instance, dry ice-0.05 M, big parallel lamellar pores were formed, resulting in overall lower pore wall density (see Fig. 3d), and additional small pores were formed on the walls (see Fig. 2d") with the consequence of the increased tortuosity, which enhances the sound absorption. Thus, less sound wave was reflected by the cryogel surface, more sound waves penetrated into the cryogel and were dissipated, finally leading to a small amount of residual sound wave (Fig. 4e). Further increasing NaCl concentration to 0.2 M, the size of the pores on the parallel lamellar walls grew too large (Fig. 2f") to increase the tortuosity and trap or consume most of the sound wave (Fig. 4f), leading to lower absorption coefficient. Therefore, the parameters, such as increasing freeze-casting temperature and increasing NaCl concentration, that facilitate and optimize the formation of large parallel lamellar pores and small side pores on the wall in pectin cryogels, could further facilitate the enhancement in sound absorption performance of pectin cryogels. In fact, the viscous and thermal layers near the pore walls, where the viscous-thermal dissipation of sound occurs, range from a thickness of approximately 10 to 350 μm, depending on the frequency [37]. This means that if the gap between two lamellas is lower than 10 μm (such as for liquid nitrogen-0 M cryogel) most of the sound cannot penetrate the material but is reflected from the surface of the material, inducing very low sound viscous-thermal dissipation in the inner pores. For dry ice-0.05 M cryogel, the gap between two lamellas is around 45 μm (23 pore walls/mm) which lies exactly in the range of viscous and thermal layers (10 to 350 μm), thus allowing the sound to penetrate into the material. Hence, the sound dissipation in the inner pores leads to higher sound absorption coefficient. Additionally, the other dimension (across the ice growth direction) of the lamellar pore can be upto 500 μm (SEM in Fig. 2d). Thus, this long and narrow shape of lamellar pores have an optimal and much better sound absorption property. When the gap between two lamellas is getting bigger (such as for dry ice-0.2 M cryogel), sound absorption is not maximal, as the sound can better transfer through the material and the effect of viscous and thermal dissipation is reduced in the inner pores. Therefore, the ability to control the optimal pore size (i.e, density of pore walls/mm) with NaCl concentration is a great advantage and enables to find the optimal density of long lamellar pores for sound absorption in the desired frequency range.

The effect of sample thickness on the sound absorption performance of pectin cryogels was further studied by using dry ice-0.05 M as an example due to its better sound absorption performance in the above description. The corresponding absorption coefficients and average absorption coefficients are presented in Fig. 4g and 4 h, respectively. As illustrated in Fig. 4g it can be observed that thickness has a significant influence on the sound absorption performance. When the sample thickness increases from 12 mm to 30 mm, the absorption coefficient has a large increase in the low frequency ranges (500–2000 Hz), while it has a slight decreasing trend in the high frequency ranges (2000–6000 Hz). The resulted average sound absorption coefficient (Fig. 4h) in the full measured frequency ranges (500–6000 Hz) could be improved with the increase of thickness. The thicker sample offers a longer sound pathway, which could provide more chances for the reflection and friction of penetrated sound waves between the lamellar pore wall; thus, resulting in more energy consumed in materials and the enhancement of sound absorption performance.

The comparison of sound absorption coefficient at different frequency of pectin cryogels with bio-based porous sound absorption materials reported earlier in the literature are summarized in Table 1. Compared with other bio-based porous sound absorption materials, freeze-casted pectin cryogels fabricated in this work present low density and higher or comparable sound absorption performance with the similar thickness. As can be noted, most of the bio-based materials studied this far are fiber-based and thus more similar in mechanical properties to glass wool (compressible and non-recoverable). Structurally, the most similar samples studied in the literature are freeze-casted cellulose II and chitosan samples.

The mechanical durability is important for sound absorption materials to expand their adaptability and scope of applications. As shown in Fig. 5a, the dry ice-0.05 M pectin cryogel with a density of 0.035 g/cm$^3$ and weight of 0.95 g could support at least 200 times of its own weight (200 g), while the glass wool, as control, with a density of 0.05 g/cm$^3$ and weight of 1.08 g has 35% compressive deformation after loading 200 g weight (Fig. S7). To quantitatively investigate the mechanical properties of freeze-casted pectin cryogels prepared with different freezing temperatures and NaCl concentrations, cryogels were tested under the uniaxial compression in the axial direction (along the ice growth direction, the same direction for sound absorption measurement). The representative stress–strain curve of pectin cryogel (dry ice-0.05 M) is shown in Fig. 5b with glass wool's stress–strain curve as a reference (see Fig. S8 for other NaCl concentrations). Pectin cryogel exhibits typical three-regime compressive behavior starting with a linear elastic deformation stage which is due to the pore wall bending. After that the elastic buckling of the pore wall under compression will show a plastic deformation plateau and material then undergoes a densification of the structure during densification region. This compressive behavior is analogous to other freeze-casted porous materials [20,28]. As can be expected, no apparent plastic deformation plateau was observed for glass wool.

The compression modulus of pectin cryogels and glass wool are shown in Fig. 5c. Clearly, the compression modulus of prepared pectin cryogels decreases with the increase of NaCl concentration except for the dry ice-0.2 M cryogel and is 300 to 700 times higher than that of glass wool thanks to the anisotropic aligned porous structures of pectin cryogels. The relatively higher compression modulus of dry ice-0.2 M cryogel comparing to dry ice-0.1 M cryogel is probably caused by the higher density (Fig. 3b). It is noteworthy that the pectin cryogel freeze-casted at −20 °C, which does not have an anisotropic structure (Fig. S2), has a compression modulus of 0.9 MPa, which is 2 to 4 times lower than that of other cryogels. This result suggests that taken mechanical properties into account, this type of cryogel is not optimal to be selected as a sound absorption material, although it has similar sound absorption property as dry ice-0.05 M sample (Fig. S9).

Although all freeze-casted pectin cryogels have anisotropic structure with aligned pore in the axial direction and most of them have similar porosity, the specific modulus is affected by their pore size (inverse of pore wall density). As shown in Fig. 5d, the specific modulus is not affected by the pore wall density for cryogels prepared without adding NaCl, however, the specific modulus decreases with the decrease of pore wall density with adding NaCl. This can be addressed to the formation of pores on the parallel lamellar structures which could weaken the plastic bending of the pore walls in the axial direction during compression. In addition, the compressive performance in the axial direction of pectin cryogels prepared in this work is better than that of other reported sound absorption porous materials [31,43–45] with an unexpectedly high specific modulus (Fig. 5e) thanks to the anisotropic aligned porous

**Table 1**
Comparison of pectin cryogels with reported bio-based sound absorption porous materials for their sound absorption coefficient at different frequency.

| Materials | Density ($g/cm^3$) | Thickness (mm) | Area density ($g/cm^2$) | Sound absorption coefficient | | | | | Ref. |
|---|---|---|---|---|---|---|---|---|---|
| | | | | 500 Hz | 1000 Hz | 2000 Hz | 4000 Hz | 6000 Hz | |
| pectin | 0.035 | 12 | 420 | 0.11 | 0.29 | 0.62 | 0.94 | 0.96 | This work |
| | | 30 | 1050 | 0.43 | 0.69 | 0.79 | 0.90 | 0.93 | |
| wood pulp fibre | 0.023 | 28 | 644 | 0.2 | 0.52 | 0.92 | 0.87 | 0.92 | [13] |
| cyclodextrin | 0.011 | 30 | 330 | 0.52 | 0.86 | 0.62 | 0.70 | 0.80 | [24] |
| cellulose II | 0.037 | 10 | 370 | 0.10 | 0.26 | 0.47 | 0.65 | 0.6 | [31] |
| chitosan | 0.034 | 30 | 1020 | 0.28 | 0.92 | 0.60 | 0.86 | 0.75 | [32] |
| sawdust/polyurethane | 0.137 | 30 | 4100 | 0.15 | 0.55 | 0.62 | 0.53 | – | [38] |
| areca nut leaf sheath fibers | 0.105 | 12 | 1260 | 0.1 | 0.13 | 0.37 | 0.50 | – | [39] |
| natural date palm fibres | 0.100 | 30 | 300 | 0.13 | 0.39 | 0.78 | 0.76 | – | [40] |
| alginate/polypropylene | 0.058 | 30 | 1740 | – | 0.59 | 0.75 | 0.78 | 0.75 | [41] |
| natural kenaf fibre | 0.031 | 30 | 930 | 0.32 | 0.26 | 0.36 | 0.55 | – | [42] |

'-' means no value was reported.

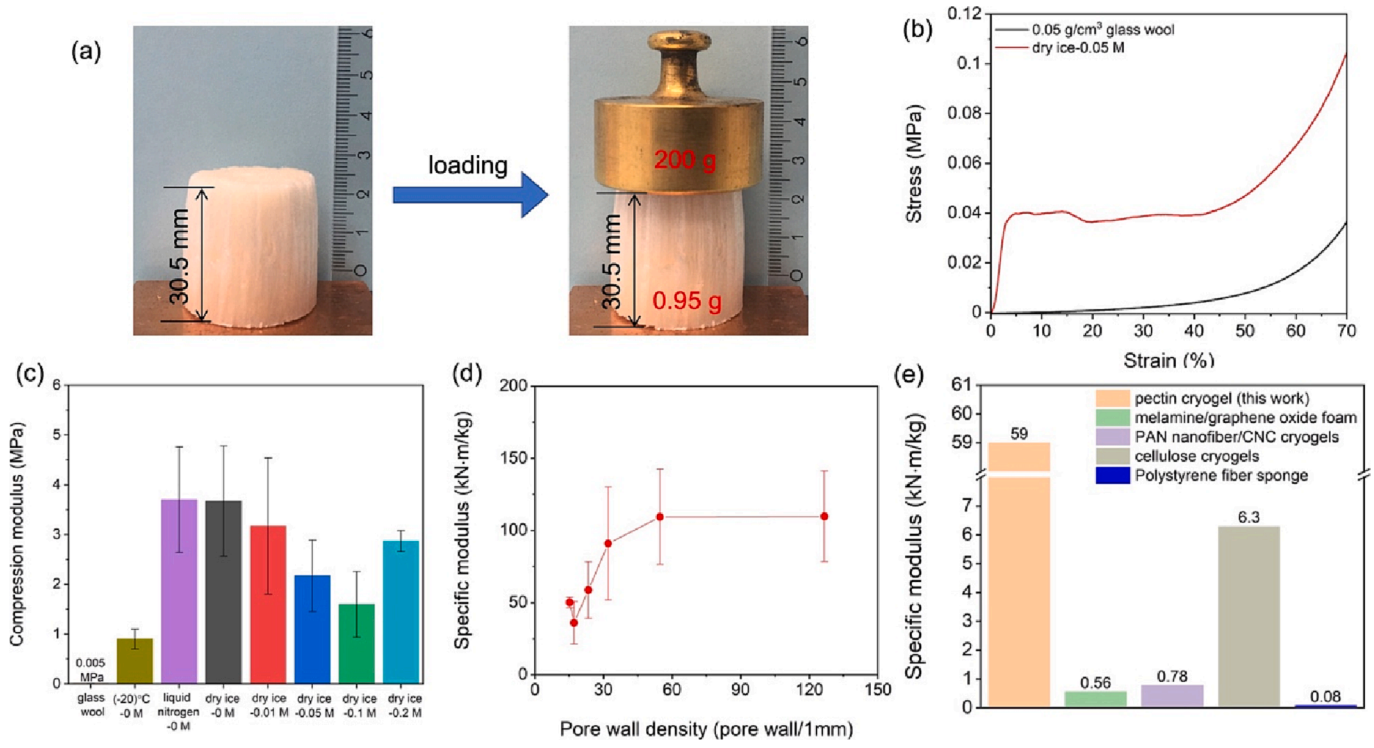


**Fig. 5.** Digital photos of pectin cryogel before and after holding 200 times its original weight (a). Compression curves of pectin cryogel (dry ice-0.05 M) and glass wool (b). Compression modulus of freeze-casted pectin cryogel prepared with different freezing sources and NaCl concentrations and glass wool (c) and pore wall density dependent of specific modulus of freeze-casted pectin cryogels (d). Comparison of pectin cryogels (dry ice-0.05 M) with reported sound absorption porous materials [31,43–45] (the detailed data about their sound absorption property is summarized in Table S1) for their specific modulus (e).

structures of pectin cryogels.

Complementary to high sound absorption property and outstanding mechanical property, the thermal insulation properties of these pectin cryogels were also investigated. The thermal conductivities of pectin cryogels in the axial direction (the same direction for sound absorption and compression measurement) were measured and summarized in Fig. 6a. The pectin cryogels have thermal conductivity around 0.032–0.049 W/(m·K) in the axial direction. Liquid nitrogen-0 M pectin cryogel has the lowest thermal conductivity and dry ice-0.1 M pectin cryogel has the highest thermal conductivity. However, the thermal conductivity in the axial direction is much higher than in the radial direction as shown in Fig. S10a (across the ice growth direction, around 0.02 W/(m·K)–0.026 W/(m·K)). This is due to the fact that the heat is directly transferred to the detection plate through the pores in the axial direction, which results in the higher thermal conductivity compared to radial direction. These results are consistent with the reported freeze-casted porous materials [23,46]. As shown in Fig. S10b, the thermal conductivity increases with the increasing temperature. In addition, pectin cryogels exhibit a pore wall density-dependency of the thermal conductivity in the axial direction (Fig. 6b). The thermal conductivity increases with the decrease of pore wall density. Lower pore wall density means bigger lamellar pores, which enable better heat transfer as compared to smaller lamellar pores. Therefore, the thermal conductivity increases with the decrease of pore wall density. This phenomenon is consistent with other porous thermal insulators in the reported literatures [47]. Interestingly, the thermal conductivity increases faster when the pore wall density is smaller than 30 pore wall/mm (Fig. 6b). This is attributed to the formation of small pores on the pore wall of the parallel lamellar structures (Fig. 2d'-2f'), which further enhances the heat transfer and results in faster increase of thermal conductivity.

The thermal insulation performance of pectin cryogel is further demonstrated by placing different thick samples on a hot or a cold plate

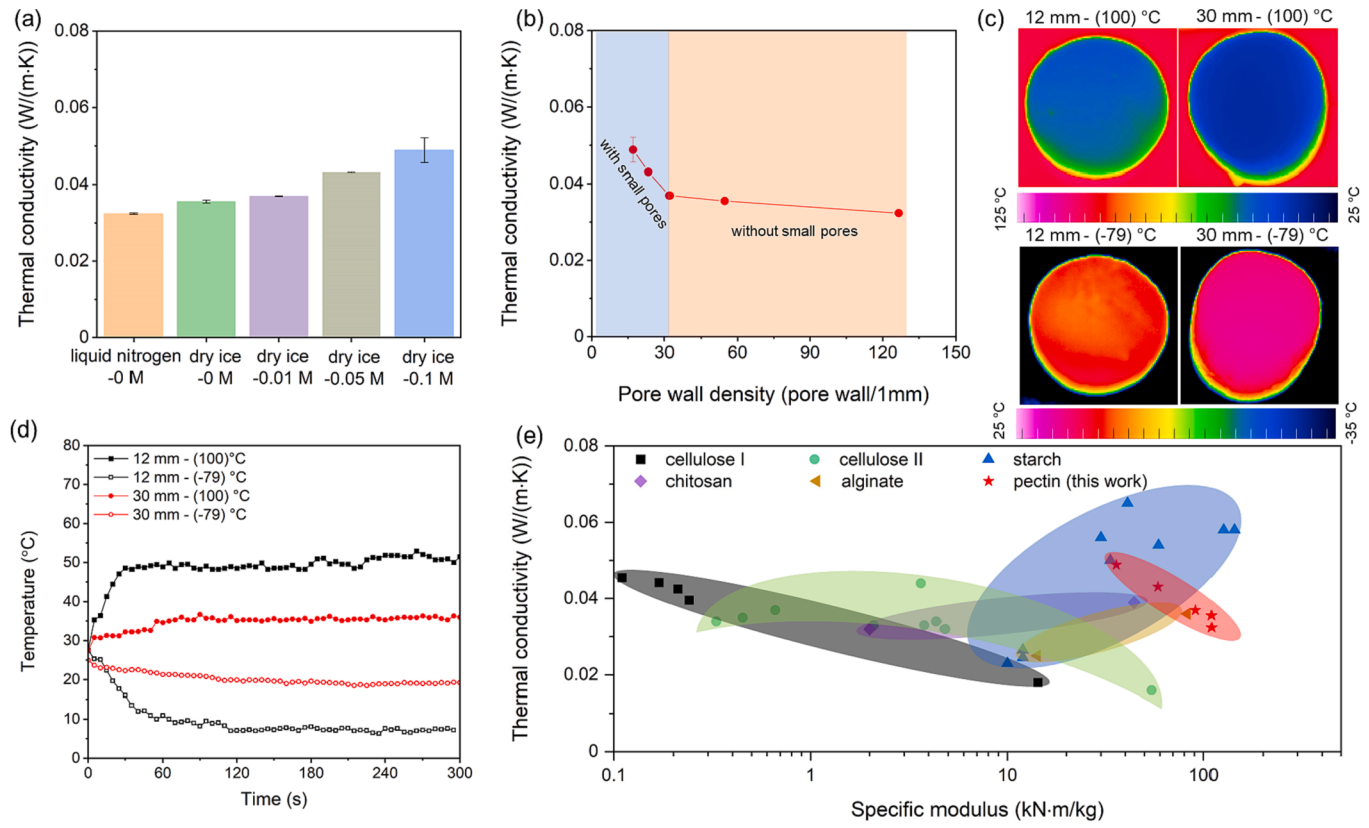


**Fig. 6.** Thermal conductivity in axial direction at 30 °C (a) and pore wall density dependency of thermal conductivity (b) of freeze-casted pectin cryogels. Infrared thermal images of pectin cryogels placed on 100 °C and –79 °C plates for 5 min (c) and the relevant maximum surface temperature as function of heating/cooling time (d) for the 12 mm and 30 mm thick dry ice-0.05 M pectin cryogels. Comparison of freeze-casted pectin cryogels with reported net polysaccharide-based porous materials [16,17,26,48–55] for their thermal conductivity as a function of the specific modulus (e).

with the temperature maintained at 100 °C or −79 °C, respectively. The sample's surface temperature was recorded every 5 s after placing it on the hot or cold plate by an infrared camera (Fig. 6c and Fig. S11). The surface temperatures as function of heating or cooling time were plotted in Fig. 6d. After heating for 5 min, the surface temperature equilibrates at 51.5 °C and 36 °C for 12 mm thick and 30 mm thick samples, respectively. Furthermore, after cooling for 5 min, the surface temperature decreases to an equilibrium at 7.2 °C and 19.2 °C for 12 mm thick and 30 mm thick samples, respectively. Therefore, pectin cryogels have a better thermal insulation property in both high and low temperature conditions. Regarding the potential applicability of these materials in the construction industry, where both high thermal and sound insulation coupled with adequate mechanical durability is required, the thermal conductivity and specific modulus of pectin cryogels have been compared with reported net polysaccharide-based porous materials [16,17,26,48–55]. As shown in Fig. 6e (the detailed data used for compiling this Figure is summarized in Table S2), the pectin cryogels show distinct advantages of high specific modulus and comparable thermal conductivity. In addition, the durability of the pectin cryogels were confirmed for the dry ice-0.05 M cryogel sample after 6 months storage at ambient conditions, which shows unaltered morphology, sound absorption performance, and mechanical property (Fig. S12). Furthermore, when taking into account that completely bio-based thermal superinsulator aerogels can be prepared from many polysaccharides [17,33,53,56,57], our future work consists of extending the current work towards exploring the performance of sound absorption of pectin cryogels at different humidity levels and building a composite of highly-performing bio-based sound absorption materials with superhydrophobicity and thermal superinsulation.

## 4. Conclusions

In this work, high-strength pectin cryogels with anisotropic structure, outstanding sound absorption, and thermal insulation properties were fabricated via a green and simple freeze-casting method. Due to the high porosity, pectin cryogels outperformed the sound absorption performance when compared to commercial sound absorption materials (glass wool) and other reported bio-based sound absorption porous materials with the similar thickness. Taken into account the lower density of pectin cryogels, the sound absorption performance of pectin cryogels is even more significant as compared to glass wool. Meanwhile, freeze-casted pectin cryogels have good mechanical properties with much higher specific compression modulus (36–110 kN·m/kg) when compared with glass wool. Additionally, the freeze-casted pectin cryogels display low thermal conductivity (0.032–0.049 W/(m·K)) and excellent thermal insulation performance.

Importantly, a wide range of pore wall densities can be produced via adding NaCl to pectin solution prior to the freeze-casting process and changing the freezing media's temperature. Meanwhile, the sound absorption property, mechanical property, and thermal conductivity exhibit a pore wall density-dependence. Increasing pore wall density (smaller anisotropic pores) leads to increase in mechanical property, decrease in thermal conductivity, and decrease in sound absorption property. Thus, optimization taking into account all these three key properties and how they depend on the morphology of the cryogels lead to maximizing sound absorption, thermal insulation, and mechanical strength of anisotropic pectin cryogels via changing the NaCl concentration. Importantly, adding NaCl enabled creation of hierarchically porous anisotropic cryogels having smaller pores on the walls of bigger lamellar pores. By adjusting the pore size (pore wall density) of the long and narrow shaped lamellar pores to the level of viscous and thermal

layers, the sound can penetrate deep into material, thus, the viscous and thermal losses in the materials are enhanced. In addition, the small pores on pore wall could increase the tortuosity which further increases sound absorption, especially at the high frequencies. This type of structure has not been reported before in the context of bio-based acoustic absorbers. Therefore, the freeze-casted pectin cryogels prepared in this work demonstrate the great potential of freeze-casted bio-based sound absorption materials to be employed as an alternative material in industrialization and construction, where development of environmentally-friendly solutions is urgently needed.

## Declaration of Competing Interest

The authors declare that they have no known competing financial interests or personal relationships that could have appeared to influence the work reported in this paper.

## Data availability

Data will be made available on request.

## Acknowledgments

This work was supported by the Academy of Finland Flagship project "FinnCERES" (Decision numbers 318890 and 318891) and "SUPER-WEAR" (Decision number: 322214). Aalto University's seed funding for ACOU-MAT project is equally acknowledged. We acknowledge Bio-Economy and RawMatTERS Finland infrastructure (RAMI) facilities based at Aalto University for measurements.

## Appendix A. Supplementary data

Supplementary data to this article can be found online at https://doi.org/10.1016/j.cej.2023.142236.

## References

[1] C. Bujoreanu, F. Nedeff, M. Benchea, M. Agop, Experimental and theoretical considerations on sound absorption performance of waste materials including the effect of backing plates, Appl. Acoust. 119 (2017) 88–93, https://doi.org/10.1016/j.apacoust.2016.12.010.

[2] T. Yu, F. Jiang, R. Zhang, M. Cao, R. Qin, C. Guo, Z. Wang, Y. Chang, Effects of volume fraction and diameter of hollow spheres on acoustic properties of metallic-hollow-sphere/polyurethane (MHSP) acoustic composites, Compos. Struct. 261 (2021), 113554, https://doi.org/10.1016/j.compstruct.2021.113554.

[3] Y. Tao, M. Ren, H. Zhang, T. Peijs, Recent progress in acoustic materials and noise control strategies – a review, Appl. Mater. Today. 24 (2021), 101141, https://doi.org/10.1016/j.apmt.2021.101141.

[4] X. Tang, X. Yan, Acoustic energy absorption properties of fibrous materials: a review, Compos. Part A Appl. Sci. Manuf. 101 (2017) 360–380, https://doi.org/10.1016/j.compositesa.2017.07.002.

[5] L. Cao, H. Shan, D. Zong, X. Yu, X. Yin, Y. Si, J. Yu, B. Ding, Fire-resistant and hierarchically structured elastic ceramic nanofibrous aerogels for efficient low-frequency noise reduction, NanoLett. 22 (2022) 1609–1617, https://doi.org/10.1021/acs.nanolett.1c04532.

[6] C. Wu, Z. Chen, F. Wang, Y. Hu, Z. Rao, E. Wang, X. Zhang, Preparation and characterization of ultralight glass fiber wool/phenolic resin aerogels with a spring-like structure, Compos. Sci. Technol. 179 (2019) 125–133, https://doi.org/10.1016/j.compscitech.2019.05.001.

[7] Q.B. Thai, R.O. Chong, P.T.T. Nguyen, D.K. Le, P.K. Le, N. Phan-Thien, H.M. Duong, Recycling of waste tire fibers into advanced aerogels for thermal insulation and sound absorption applications, J. Environ. Chem. Eng. 8 (2020) 104279. https://doi.org/10.1016/j.jece.2020.104279.

[8] V.G. Krishnan, A.M. Joseph, S. Kuzhichalil Peethambharan, E.B. Gowd, Nanoporous crystalline aerogels of syndiotactic polystyrene: polymorphism, dielectric, thermal, and acoustic properties, Macromolecules 54 (2021) 10605–10615, https://doi.org/10.1021/acs.macromol.1c01555.

[9] L. Shen, H. Zhang, Y. Lei, Y. Chen, M. Liang, H. Zou, Hierarchical pore structure based on cellulose nanofiber/melamine composite foam with enhanced sound absorption performance, Carbohydr. Polym. 255 (2021), 117405, https://doi.org/10.1016/j.carbpol.2020.117405.

[10] H. Choe, G. Sung, J.H. Kim, Chemical treatment of wood fibers to enhance the sound absorption coefficient of flexible polyurethane composite foams, Compos. Sci. Technol. 156 (2018) 19–27, https://doi.org/10.1016/j.compscitech.2017.12.024.

[11] J.H. Oh, H.R. Lee, S. Umrao, Y.J. Kang, I.K. Oh, Self-aligned and hierarchically porous graphene-polyurethane foams for acoustic wave absorption, Carbon 147 (2019) 510–518, https://doi.org/10.1016/j.carbon.2019.03.025.

[12] E. Taban, P. Soltani, U. Berardi, A. Putra, S.M. Mousavi, M. Faridan, S.E. Samaei, A. Khavanin, Measurement, modeling, and optimization of sound absorption performance of Kenaf fibers for building applications, Build. Environ. 180 (2020), 107087, https://doi.org/10.1016/j.buildenv.2020.107087.

[13] J. Cucharero, S. Ceccherini, T. Maloney, T. Lokki, T. Hänninen, Sound absorption properties of wood-based pulp fibre foams, Cellul. 28 (2021) 4267–4279, https://doi.org/10.1007/s10570-021-03774-1.

[14] E. Taban, A. Tajpoor, M. Faridan, S.E. Samaei, M.H. Beheshti, Acoustic absorption characterization and prediction of natural coir fibers, Acoust. Aust. 47 (2019) 67–77, https://doi.org/10.1007/s40857-019-00151-8.

[15] C. He, J. Huang, S. Li, K. Meng, L. Zhang, Z. Chen, Y. Lai, Mechanically resistant and sustainable cellulose-based composite aerogels with excellent flame retardant, sound-absorption, and superantiwetting ability for advanced engineering materials, ACS Sustain. Chem. Eng. 6 (2018) 927–936, https://doi.org/10.1021/acssuschemeng.7b03281.

[16] J. Feng, D. Le, S.T. Nguyen, V. Tan Chin Nien, D. Jewell, H.M. Duong, Silica–cellulose hybrid aerogels for thermal and acoustic insulation applications, Colloids Surfaces A Physicochem Eng. Asp. 506 (2016) 298–305.

[17] J. Jaxel, G. Markevicius, A. Rigacci, T. Budtova, Thermal superinsulating silica aerogels reinforced with short man-made cellulose fibers, Compos. Part A Appl. Sci. Manuf. 103 (2017) 113–121, https://doi.org/10.1016/j.compositesa.2017.09.018.

[18] G. Shao, D.A.H. Hanaor, X. Shen, A. Gurlo, Freeze casting: from low-dimensional building blocks to aligned porous structures—a review of novel materials, methods, and applications, Adv. Mater. 32 (2020) 1907176, https://doi.org/10.1002/adma.201907176.

[19] K.L. Scotti, D.C. Dunand, Freeze casting – a review of processing, microstructure and properties via the open data repository, freezecasting.net, Prog. Mater. Sci. 94 (2018) 243–305, https://doi.org/10.1016/j.pmatsci.2018.01.001.

[20] S. Christoph, A. Hamraoui, E. Bonnin, C. Garnier, T. Coradin, F.M. Fernandes, Ice-templating beet-root pectin foams: controlling texture, mechanics and capillary properties, Chem. Eng. J. 350 (2018) 20–28, https://doi.org/10.1016/j.cej.2018.05.160.

[21] K. Qiu, U.G.K. Wegst, Excellent specific mechanical and electrical properties of anisotropic freeze-cast native and carbonized bacterial cellulose-alginate foams, Adv. Funct. Mater. 32 (1) (2022) 2105635.

[22] Z.L. Yu, N. Yang, L.C. Zhou, Z.Y. Ma, Y.B. Zhu, Y.Y. Lu, B. Qin, W.Y. Xing, T. Ma, S. C. Li, H.L. Gao, H.A. Wu, S.H. Yu, Bioinspired polymeric woods, Sci. Adv. 4 (2018), https://doi.org/10.1126/sciadv.aat7223.

[23] W. Xiao, P. Wang, X. Song, B. Liao, K. Yan, J.J. Zhang, Facile fabrication of anisotropic chitosan aerogel with hydrophobicity and thermal superinsulation for advanced thermal management, ACS Sustain. Chem. Eng. 9 (2021) 9348–9357, https://doi.org/10.1021/acssuschemeng.1c02217.

[24] Z.J. Nie, J.X. Wang, C.Y. Huang, J.F. Feng, S.T. Fan, M. Tan, C. Yang, B.J. Li, S. Zhang, Hierarchically and wood-like cyclodextrin aerogels with enhanced thermal insulation and wide spectrum acoustic absorption, Chem. Eng. J. 446 (2022), 137280, https://doi.org/10.1016/j.cej.2022.137280.

[25] Y. Zhou, S. Fu, Y. Pu, S. Pan, A.J. Ragauskas, Preparation of aligned porous chitin nanowhisker foams by directional freeze-casting technique, Carbohydr. Polym. 112 (2014) 277–283, https://doi.org/10.1016/j.carbpol.2014.05.062.

[26] B. Wicklein, A. Kocjan, G. Salazar-Alvarez, F. Carosio, G. Camino, M. Antonietti, L. Bergström, Thermally insulating and fire-retardant lightweight anisotropic foams based on nanocellulose and graphene oxide, Nat. Nanotechnol. 10 (2015) 277–283, https://doi.org/10.1038/nnano.2014.248.

[27] J. Shan, D. Liu, F. Su, M. Li, H. Tian, M. Guo, W. Qiao, J. He, Q. Li, J. Qian, Anisotropic structure and properties of chitin and chitosan nanofibril-supported starch foams, ACS Sustain. Chem. Eng. 8 (2020) 17387–17396, https://doi.org/10.1021/acssuschemeng.0c05484.

[28] B. Chen, Q. Zheng, J. Zhu, J. Li, Z. Cai, L. Chen, S. Gong, Mechanically strong fully biobased anisotropic cellulose aerogels, RSC Adv. 6 (2016) 96518–96526, https://doi.org/10.1039/c6ra19280g.

[29] M.C.N. Picot-Allain, B. Ramasawmy, M.N. Emmambux, Extraction, characterisation, and application of pectin from tropical and sub-tropical fruits: a review, Food Rev. Int. 38 (3) (2022) 282–312.

[30] F. Zou, H. Li, Y. Dong, G.C. Tewari, J. Vapaavuori, Optically transparent pectin/poly(methyl methacrylate) composite with thermal insulation and UV blocking properties based on anisotropic pectin cryogel, Chem. Eng. J. 439 (2022), 135738, https://doi.org/10.1016/j.cej.2022.135738.

[31] C.W. Lou, X. Zhou, X. Liao, H. Peng, H. Ren, T.T. Li, J.H. Lin, Sustainable cellulose-based aerogels fabricated by directional freeze-drying as excellent sound-absorption materials, J. Mater. Sci. 56 (2021) 18762–18774, https://doi.org/10.1007/s10853-021-06498-6.

[32] X. Jiang, J. Zhang, F. You, C. Yao, H. Yang, R. Chen, Chitosan/clay aerogel : microstructural evolution, flame resistance and sound absorption, Appl. Clay Sci. 228 (2022), 106624, https://doi.org/10.1016/j.clay.2022.106624.

[33] S. Groult, T. Budtova, Thermal conductivity/structure correlations in thermal super-insulating pectin aerogels, Carbohydr. Polym. 196 (2018) 73–81, https://doi.org/10.1016/j.carbpol.2018.05.026.

[34] S. Wu, C. Zhu, Z. He, H. Xue, Q. Fan, Y. Song, J.S. Francisco, X.C. Zeng, J. Wang, Ion-specific ice recrystallization provides a facile approach for the fabrication of porous materials, Nat. Commun. 8 (2017) 1–8, https://doi.org/10.1038/ncomms15154.

[35] Y. Chen, F. Yuan, Q. Su, C. Yu, K. Zhang, P.P. Luo, D. Hu, Y. Guo, A novel sound absorbing material comprising discarded luffa scraps and polyester fibers, J. Clean. Prod. 245 (2020), 118917, https://doi.org/10.1016/j.jclepro.2019.118917.
[36] K. Pang, X. Liu, J. Pang, A. Samy, J. Xie, Y. Liu, L. Peng, Z. Xu, C. Gao, Highly efficient cellular acoustic absorber of graphene ultrathin drums, Adv. Mater. 34 (2022) 1–9, https://doi.org/10.1002/adma.202103740.
[37] M. Berggren, A. Bernland, D. Noreland, Acoustic boundary layers as boundary conditions, J. Comput. Phys. 371 (2018) 633–650, https://doi.org/10.1016/j.jcp.2018.06.005.
[38] A.E. Tiuc, O. Nemeş, H. Vermeşan, A.C. Toma, New sound absorbent composite materials based on sawdust and polyurethane foam, Compos. Part B Eng. 165 (2019) 120–130, https://doi.org/10.1016/j.compositesb.2018.11.103.
[39] M. Raj, S. Fatima, N. Tandon, A study of areca nut leaf sheath fibers as a green sound-absorbing material, Appl. Acoust. 169 (2020), 107490, https://doi.org/10.1016/j.apacoust.2020.107490.
[40] E. Taban, A. Khavanin, A. Ohadi, A. Putra, A.J. Jafari, M. Faridan, A. Soleimanian, Study on the acoustic characteristics of natural date palm fibres: experimental and theoretical approaches, Build. Environ. 161 (2019), 106274, https://doi.org/10.1016/j.buildenv.2019.106274.
[41] A.G.M. Pornea, J.M.C. Puguan, J.L.A. Ruello, H. Kim, Multifunctional dual-pore network aerogel composite material for broadband sound absorption, thermal insulation, and fire repellent applications, ACS Appl. Polym. Mater. 4 (2022) 2880–2895, https://doi.org/10.1021/acsapm.2c00139.
[42] Z.Y. Lim, A. Putra, M.J.M. Nor, M.Y. Yaakob, Sound absorption performance of natural kenaf fibres, Appl. Acoust. 130 (2018) 107–114, https://doi.org/10.1016/j.apacoust.2017.09.012.
[43] M.J. Nine, M. Ayub, A.C. Zander, D.N.H. Tran, B.S. Cazzolato, D. Losic, Graphene oxide-based lamella network for enhanced sound absorption, Adv. Funct. Mater. 27 (2017) 1–10, https://doi.org/10.1002/adfm.201703820.
[44] L. Cao, Y. Si, X. Yin, J. Yu, B. Ding, Ultralight and resilient electrospun fiber sponge with a lamellar corrugated microstructure for effective low-frequency sound absorption, ACS Appl. Mater. Interfaces. 11 (2019) 35333–35342, https://doi.org/10.1021/acsami.9b12444.
[45] L. Cao, X. Yu, X. Yin, Y. Si, J. Yu, B. Ding, Hierarchically maze-like structured nanofiber aerogels for effective low-frequency sound absorption, J. Colloid Interface Sci. 597 (2021) 21–28, https://doi.org/10.1016/j.jcis.2021.03.172.
[46] X. Zhang, X. Zhao, T. Xue, F. Yang, W. Fan, T. Liu, Bidirectional anisotropic polyimide/bacterial cellulose aerogels by freeze-drying for super-thermal insulation, Chem. Eng. J. 385 (2020), 123963, https://doi.org/10.1016/j.cej.2019.123963.
[47] S.F. Plappert, J.M. Nedelec, H. Rennhofer, H.C. Lichtenegger, F.W. Liebner, Strain hardening and pore size harmonization by uniaxial densification: a facile approach toward superinsulating aerogels from nematic nanofibrillated 2,3-dicarboxyl cellulose, Chem. Mater. 29 (2017) 6630–6641, https://doi.org/10.1021/acs.chemmater.7b00787.
[48] Y. Wang, K. Uetani, S. Liu, X. Zhang, Y. Wang, P. Lu, T. Wei, Z. Fan, J. Shen, H. Yu, S. Li, Q. Zhang, Q. Li, J. Fan, N. Yang, Q. Wang, Y. Liu, J. Cao, J. Li, W. Chen, Multifunctional bionanocomposite foams with a chitosan matrix reinforced by nanofibrillated cellulose, ChemNanoMat. 3 (2017) 98–108, https://doi.org/10.1002/cnma.201600266.
[49] M. Cao, B.W. Liu, L. Zhang, Z.C. Peng, Y.Y. Zhang, H. Wang, H.B. Zhao, Y.Z. Wang, Fully biomass-based aerogels with ultrahigh mechanical modulus, enhanced flame retardancy, and great thermal insulation applications, Compos. Part B Eng. 225 (2021), 109309, https://doi.org/10.1016/j.compositesb.2021.109309.
[50] K. Shang, W. Liao, J. Wang, Y.T. Wang, Y.Z. Wang, D.A. Schiraldi, Nonflammable alginate nanocomposite aerogels prepared by a simple freeze-drying and post-cross-linking method, ACS Appl. Mater. Interfaces. 8 (2016) 643–650, https://doi.org/10.1021/acsami.5b09768.
[51] J. Qi, Y. Xie, H. Liang, Y. Wang, T. Ge, Y. Song, M. Wang, Q. Li, H. Yu, Z. Fan, S. Liu, Q. Wang, Y. Liu, J. Li, P. Lu, W. Chen, Lightweight, flexible, thermally-stable, and thermally-insulating aerogels derived from cotton nanofibrillated cellulose, ACS Sustain. Chem. Eng. 7 (2019) 9202–9210, https://doi.org/10.1021/acssuschemeng.8b06851.
[52] J. Fan, S. Ifuku, M. Wang, K. Uetani, H. Liang, H. Yu, Y. Song, X. Li, J. Qi, Y. Zheng, H. Wang, J. Shen, X. Zhang, Q. Li, S. Liu, Y. Liu, Q. Wang, J. Li, P. Lu, Z. Fan, W. Chen, Robust nanofibrillated cellulose hydro/aerogels from benign solution/solvent exchange treatment, ACS Sustain. Chem. Eng. 6 (2018) 6624–6634, https://doi.org/10.1021/acssuschemeng.8b00418.
[53] L. Druel, R. Bardl, W. Vorwerg, T. Budtova, Starch aerogels: a member of the family of thermal superinsulating materials, Biomacromolecules. 18 (2017) 4232–4239, https://doi.org/10.1021/acs.biomac.7b01272.
[54] F. Zou, J. Bouvard, C. Pradille, T. Budtova, Ice-templated additive-free porous starches with tuned morphology and properties, Eur. Polym. J. 176 (2022), 111403, https://doi.org/10.1016/j.eurpolymj.2022.111403.
[55] J. Zhu, R. Xiong, F. Zhao, T. Peng, J. Hu, L. Xie, H. Xie, K. Wang, C. Jiang, Lightweight, high-strength, and anisotropic structure composite aerogel based on hydroxyapatite nanocrystal and chitosan with thermal insulation and flame retardant properties, ACS Sustain. Chem. Eng. 8 (2020) 71–83, https://doi.org/10.1021/acssuschemeng.9b03953.
[56] C. Rudaz, R. Courson, L. Bonnet, S. Calas-Etienne, H. Sallée, T. Budtova, Aeropectin: fully biomass-based mechanically strong and thermal superinsulating aerogel, Biomacromolecules. 15 (2014) 2188–2195, https://doi.org/10.1021/bm500345u.
[57] F. Zou, T. Budtova, Polysaccharide-based aerogels for thermal insulation and superinsulation: an overview, Carbohydr. Polym. 266 (2021), 118130, https://doi.org/10.1016/j.carbpol.2021.118130.